Growth and properties of $SrAl_2O_4$: Eu, *Re* single-crystals: Effects of rare earths on a long-persistent phosphor

T. Ishibashi, S. Furukawa, H. Oda and A. Yamanaka*
Department of Opto-Electronic System Engineering,
Chitose Institute of Science and Technology,
758-65 Bibi, Chitose, Hokkaido, 066-8655, Japan
a-yamana@photon.chitose.ac.jp

Single-crystals of $SrAl_2O_4$: Eu, *Re* (*Re*: rare earths) have been grown by the floating-zone method. It is found that their optical properties are less sensitive to *Re*: The absorption edge is located at the same wavelength with that of $SrAl_2O_4$: Eu, and the luminescence properties are primarily governed by 5*d*-4*f* transition of Eu^{2+}. On the other hand, the temporal evolution of the emissions depends on *Re*, demonstrating that the Re^{3+} plays a key role for an electron-trap.
Key words: $SrAl_2O_4$, long-persistent phosphor, floating zone method,

1. INTRODUCTION

$SrAl_2O_4$ has received attractive much attention, because the intense green-emission form Eu^{2+} exhibits extremely long afterglow by co-doping of Dy^{3+} or Nd^{3+} [1]. These long-persistent phosphors, which do not include radioactive elements such as ^{147}Pm, can be used safely as the phosphorous pigments not only for the luminous watches and clocks but also for the emergency-exit-signs applications. Although the great number of researches has been reported, the most of the studies have been focused on $SrAl_2O_4$: Eu, Dy or $SrAl_2O_4$: Eu, Nd [2,3]. To clarify the mechanism of the long afterglow, detail optical measurements in $SrAl_2O_4$:Eu, *Re* are critically important. Considering this situation in mind, we have attempted to grow single-crystals of $SrAl_2O_4$, doped with and co-doped with several rare earth elements. In this paper, we report the results of optical measurements in $SrAl_2O_4$: Eu, *Re* single-crystals.

2. CRYSTAL GROWTH

Figure 1 shows single-crystals, grown in a floating-zone furnace equipped with a Xe-discharge lamp (Canon Machinery Inc., SC-M50XS). Dimension of the as-grown crystals was 20~40 mm long and 3~5 mm in diameter. Powder XRD patterns of these samples are essentially the same as nominally pure $SrAl_2O_4$, being consistent with the β-tridymite structure [4].

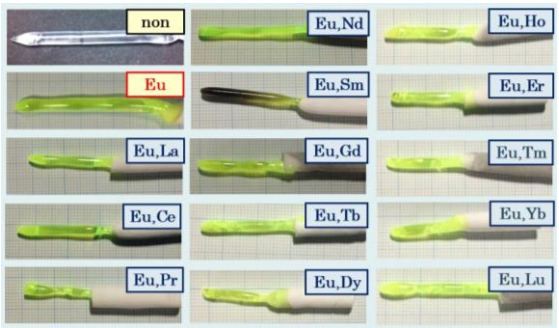

Figure 1. Single-crystals of $SrAl_2O_4$ and $SrAl_2O_4$: Eu and $SrAl_2O_4$: Eu, *Re*.

Starting materials of the samples were $SrAl_2O_4$, α-Al_2O_3 and rare earth oxides. Concentrations of both Eu and *Re* were fixed o be 1.0 %. Appropriate amount of theses powders was well mixed and pressed into a rod shape. The rod was sintered in air at 1000 ºC. During the melting process, Ar(92%)-H_2(8%) gas was flown to reduce excess oxygens in starting material of Eu_2O_3.

3. RESULTS AND DISCUSSIONS

3.1 Optical Transmission

The transmission spectra of $SrAl_2O_4$: Eu, *Re* are shown in Figure 2, where the spectrum (red line) of nominally pure $SrAl_2O_4$ is also plotted for comparison. These spectra were measured in the disc-shape samples with the thickness of ~1.5 mm, prepared from the single-crystalline rod shown in Figure 1. Both sides of the disk have been polished. We immediately find that the transmission spectrum is less sensitive to *Re*. That is, $SrAl_2O_4$: Eu, *Re* commonly exhibits an absorption edge at about 450 nm and is transparent up to 3000 nm. This profile is essentially the same as that of $SrAl_2O_4$: Eu. On the other hand, nominally pure $SrAl_2O_4$ is transparent above 200 nm, indicating a wide band gap of the host material. Therefore, the strong absorption band between 200 nm and 450 nm should be due to the 4*f*-5*d* transitions in a divalent Eu^{2+}. In this connection, it is important to note that co-doped *Re* leads to no significant absorption at least up to 3000 nm.

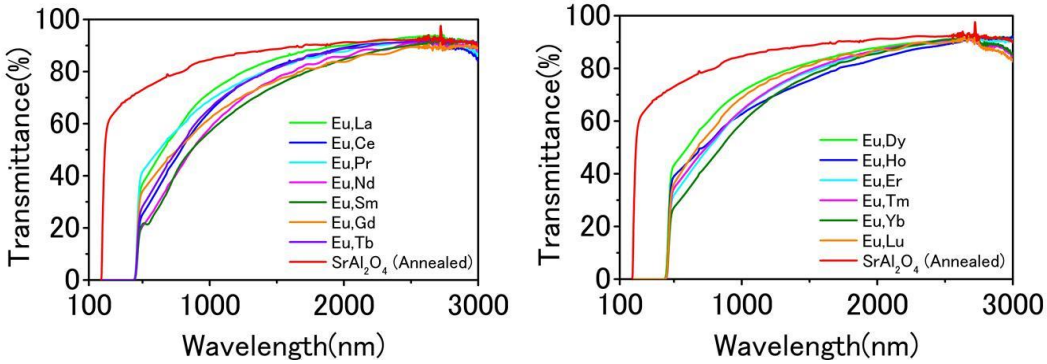

Figure 2. Optical transmission spectra of $SrAl_2O_4$: Eu, *Re*. Left: La, Ce, Pr, Nd, Sm, Gd, Tb. Right: Dy, Ho, Er, Tm, Yb, Lu. The red line is the spectrum of non-doped $SrAl_2O_4$.

3.2 Luminescence

Figure 3 illustrates the photoluminescence spectra of $SrAl_2O_4$: Eu, *Re*, where the excitation wavelength is 365 nm. All samples shows the intense yellow-green emissions, the spectral profile of which is nearly identical to that of $SrAl_2O_4$: Eu. Evidently, the 5*d*-4*f* transitions of Eu^{2+} primarily govern the photoluminescence in $SrAl_2O_4$: Eu, *Re*.

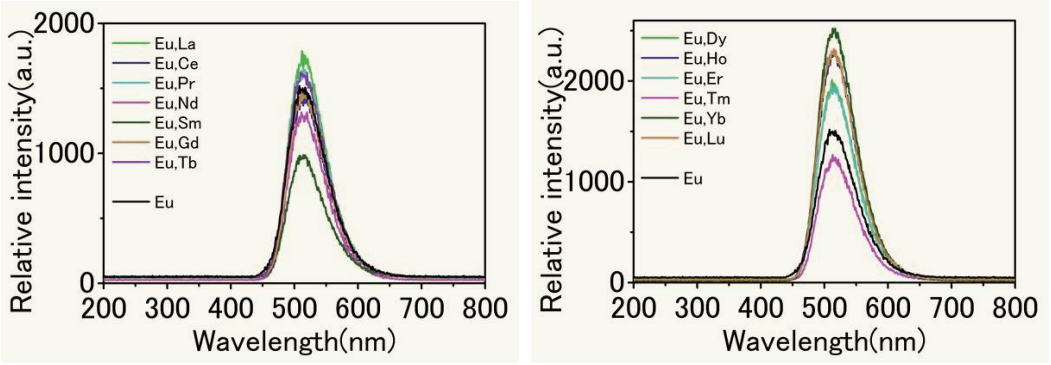

Figure 3. Photoluminescence spectra of $SrAl_2O_4$: Eu, *Re*. Left: La, Ce, Pr, Nd, Sm, Gd, Tb. Right: Dy, Ho, Er, Tm, Yb, Lu. The wavelength of excitation light is 365 nm.

3.3 Afterglow

Figures 4 and 5 display the images of the disk-shape single-crystals of $SrAl_2O_4$: Eu, *Re* and temporal evolution of the emission intensity, respectively. As shown in the upper figure of Figure 4, all samples emit green luminescence under continuous illumination of UV-light with the wavelength of 365 nm. The brightness is not very different among them, as expected from the photoluminescence spectra shown in Figure 3. When we stop the UV-illumination, we find all samples emitting the afterglow (bottom figure of Figure 4). Evidently, the bright afterglow manifests itself in Nd, Dy, Ho and Yb co-doped samples.

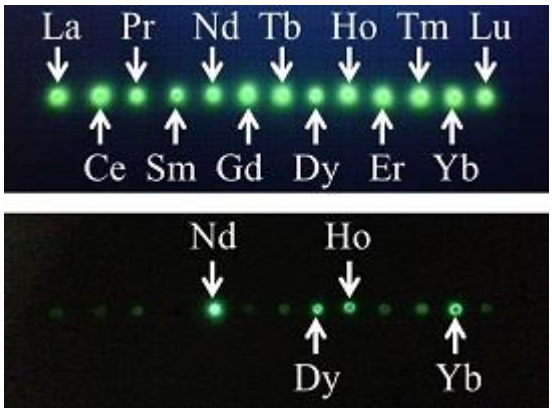

Figure 4. Image of the disk-shape samples $SrAl_2O_4$: Eu, *Re*, (top) under illuminating of 365 nm light and (bottom) at 10 seconds after illumination stop.

The time-dependence of the emission intensity shown in Figure 5 clearly demonstrates that co-doping of Nd gives rise to the bright afterglow up to 1000 seconds. However, the Dy co-doping is effective for the long-persistent phosphors applications, because the temporal behavior of $SrAl_2O_4$: Eu, Dy is more gradual than others. In Ho and Yb co-doped samples, the temporal evolution is comparable to that in Dy co-doped samples, but the intensity is about 30 % at 1000 seconds.

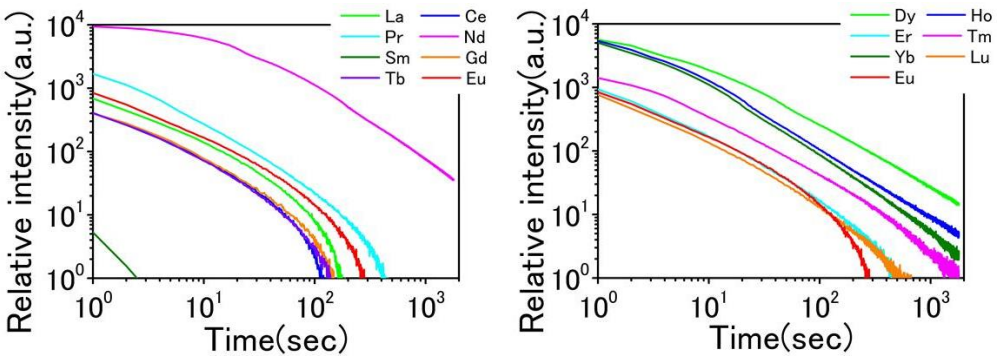

Figure 5. Temporal evolution of the emission intensity from $SrAl_2O_4$: Eu, *Re*. Left: La, Ce, Pr, Nd, Sm, Gd, Tb. Right: Dy, Ho, Er, Tm, Yb, Lu. The intensity of $SrAl_2O_4$: Eu is plotted as the red line in both figures.

3.4 Discussions

According to the Dorenbos model [5,6], the photo-excited electron is the 5*d* level of Eu^{2+} moves to a trivalent Re^{3+} through the conduction band of host $SrAl_2O_4$, and, then, forms a divalent Re^{2+}. Thermal energy is required to release the trapped electron, after which it recombines upon reaching a luminescent Eu^{2+}. Thus the energy of a divalent Re^{2+} relative to that of the conduction band is crucial for the

long-persistent phosphors. A recent theoretical calculation [7] has reported that the divalent Nd^{2+} and Ho^{2+} have nearly the same energy with that of Dy^{2+}, being basically consistent with the present results. The afterglow in $SrAl_2O_4$: Eu, Yb might be related to Yb^{+}, since Yb^{2+} has a deeper energy level in $SrAl_2O_4$.

It is important to note that other rare earth co-doped samples show tendency of the afterglow, as can be seen in Figure 5. It turns out that their temporal evolution is comparable to that observed in $SrAl_2O_4$: Eu. This fact implies that the mechanism of the long-persistent phosphorescence is not so simple. Indeed, our investigation has revealed the existence of the electron-trapping states in $SrAl_2O_4$: Eu by the UV-induced infrared absorption [8].

4. SUMMARY

We have successfully grown single-crystals of $SrAl_2O_4$: Eu, *Re*. We find that these compounds commonly have the absorption edge at about 450 nm and exhibit the intense green photoluminescence, resulted from the 5*d*-4*f* transition of Eu^{2+}. In contrast of these properties, the afterglow depends significantly on co-doped rare earth *Re*. These results are basically consistent with the Dorenbos model for the long-persistent phosphors.

REFERENCES

[1] T. Matsuzawa, Y. Aoki, N. Takeuchi and Y. Murayama, J. Electrochem. Soc., **143**, 2670 (1996).
[2] P. F. Smet, K. Van den Eeckhout, O. Q. De Clercq, and D. Poelman, Materials, **3**, 2536 (2010).
[3] K. Van den Eeckhout, P. F. Smet and D. Poelman, *Materials*, **3**, 2536 (2010).
[4] M. Avdeeva, S. Yakovleva, A. A. Yaremchenkob, and V. V. Khartonb, J. Solid State Chem., **180**, 3535 (2007).
[5] P. Dorenbos, J. Electrochem. Soc., **152**, H107–H110 (2005).
[6] P. Dorenbos, J. Phys. Condens. Matter **17**, 8103–8111 (2005).
[7] J. Botterman, J. J. Joos, and P. F. Smet, Phys. Rev. **B90**, 085147 (2014).
[8] Y. Tsurumi, M. Kitaura, A. Ohnishi, T. Ishibashi, S. Furukawa, H. Oda and A. Yamanaka, UVSOR Activity Report 2016, III-2. Material Sciences, 74 (2016).